

Coupled responses between a ship and recessed moonpools

Junxuan Chen*, Xinshu Zhang†

State Key Laboratory of Ocean Engineering, Shanghai Jiao Tong University, Shanghai 200240, China

Highlights

- Dedicated experiments were performed to investigate the coupled hydrodynamic behavior of the ship with a recessed moonpool under regular waves and irregular white-noise waves.
- It is found that as the recess length increases, the effect of piston-mode resonance on the heave motion becomes less significant, while its effect on the surge motion becomes more pronounced in head waves.

1 Introduction

A moonpool refers to a vertical opening in ships or offshore platforms. When the frequencies of incident waves or ship motion approach the natural frequency of the moonpool, the amplitude of the free-surface response inside the moonpool increases significantly, which may lead to slamming and green-water phenomena. Predicting the natural frequencies of moonpool resonance, including piston and sloshing modes, is critical. Numerous studies have been performed to predict natural frequencies for two-dimensional and three-dimensional moonpools without recesses (Molin, 2001; Molin *et al.*, 2018; Zhang *et al.*, 2019).

Recent moonpool designs incorporate recess structures for the installation of subsea equipment. Molin (2017) developed a novel model to evaluate the natural frequencies of the recessed moonpool. Zhang & Li (2022) proposed semi-analytical models to compute the natural frequencies and modal shapes for three-dimensional moonpools both with and without recesses. Xu *et al.* (2020) used WAMIT to compute the natural frequencies of moonpools in fixed and free-floating conditions. They found that natural frequencies of moonpools in free-floating conditions are somehow different from those in fixed conditions, which can be attributed to the coupling effect between the ship and the moonpool. To investigate the coupled dynamics between different sizes of moonpools and a ship, Senthuram *et al.* (2020) performed experiments on a ship with clean moonpools (i.e., without recesses) of different dimensions in an ocean wave basin.

Most of the studies mentioned above have focused on a clean moonpool, with limited research on the coupled responses between a ship and a recessed moonpool. The effect of a recessed moonpool on ship motion is not well understood. In the present study, model tests were conducted in the Ocean Wave Basin of Shanghai Jiao Tong University to investigate the influence of recesses on coupled dynamics.

2 Experimental set-up

Dedicated experiments were carried out in the Ocean Wave Basin, which measures 50 m in length, 40 m in width, and has a water depth of 8 m during the experiments. Flap-hinged wave generators are installed along

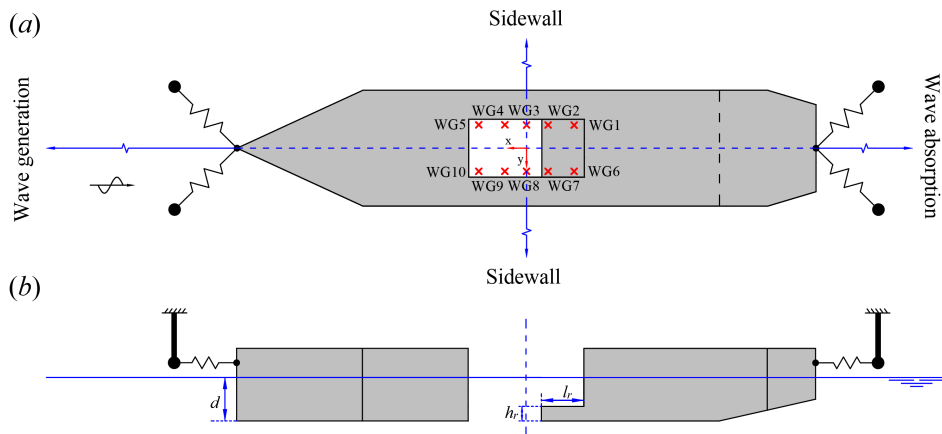


Figure 1: Sketch of the ship model with a recessed moonpool in the wave basin. (a) Top view. (b) Side view.

*Presenting author

†xinshuz@sjtu.edu.cn

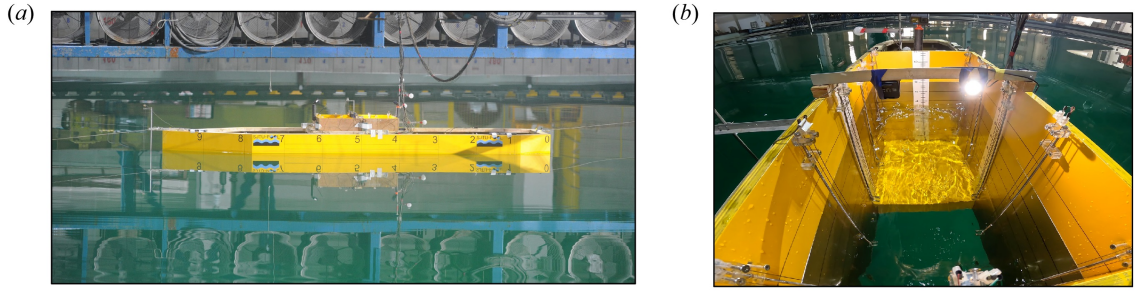


Figure 2: The ship model and the moonpool. (a) A snapshot of the ship model with a soft-mooring system ; (b) A snapshot of video recordings of the moonpool response inside RMP4.

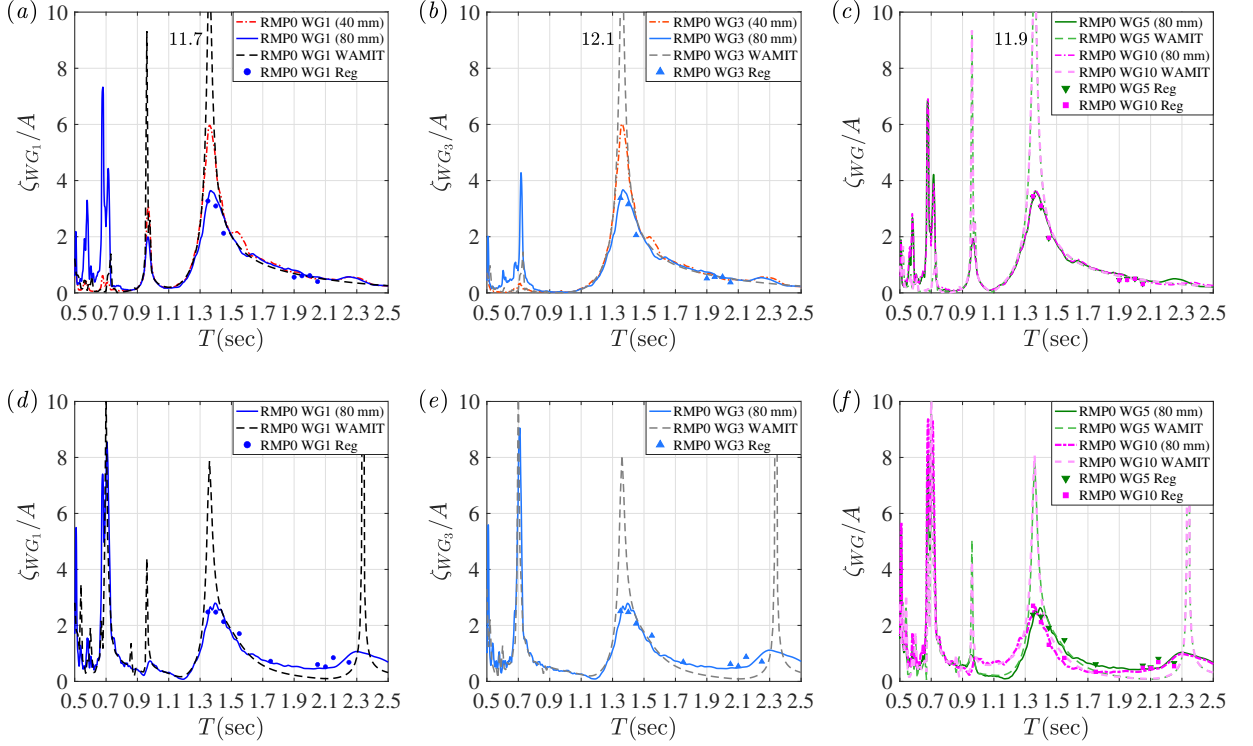


Figure 3: Free-surface elevation RAOs inside RMP0: (a) WG1, head wave; (b) WG3, head wave; (c) WG5 and WG10, head wave; (d) WG1, beam wave; (e) WG3, beam wave; (f) WG5 and WG10, beam wave. A denotes the amplitude of the incident wave.

two adjacent sides of the basin, and wave-absorbing beaches are installed on the opposite sides to minimize wave reflections. In the present study, the free-surface responses within the moonpool and the motions of the ship were recorded.

The ship model is 4 m in length, 0.8 m in width, and 0.3 m in draft, with a scale ratio of 1:40. As shown in Fig. 1, the origin of the coordinate system is set at the center of the moonpool, positioned on the horizontal plane. A total of ten wave gauges are placed inside the moonpool, five on each side. Four recessed moonpools were tested in the experiments. RMP0, RMP2, RMP3, and RMP4 represent moonpools with recess lengths of 0, 0.2, 0.3 and 0.4 m, respectively. In addition, a ship model without a moonpool (denoted as NMP) was tested in the experiments for comparison of motion response.

Photos of the ship model, placed at the center of the wave basin, along with the soft-mooring system, are shown in Fig. 2. Cameras were placed above the moonpool for video recording. Experiments were conducted under white-noise irregular waves with significant wave heights of $H_s = 40$ mm and $H_s = 80$ mm. Regular waves of different periods with a wave steepness of $H/\lambda = 1/80$ were utilized, where H represents the wave height and λ denotes the wavelength of the incident wave.

3 Results

Experimental results are compared with the free-surface response and ship motion RAOs obtained using the wave diffraction/radiation code WAMIT. The natural periods of the moonpool were determined by analyzing the RAO curves and modal shapes derived from the results of white-noise irregular wave tests.

Fig. 3 illustrates the free-surface response at WG1, WG3, WG5 and WG10 inside RMP0 (without a recess)

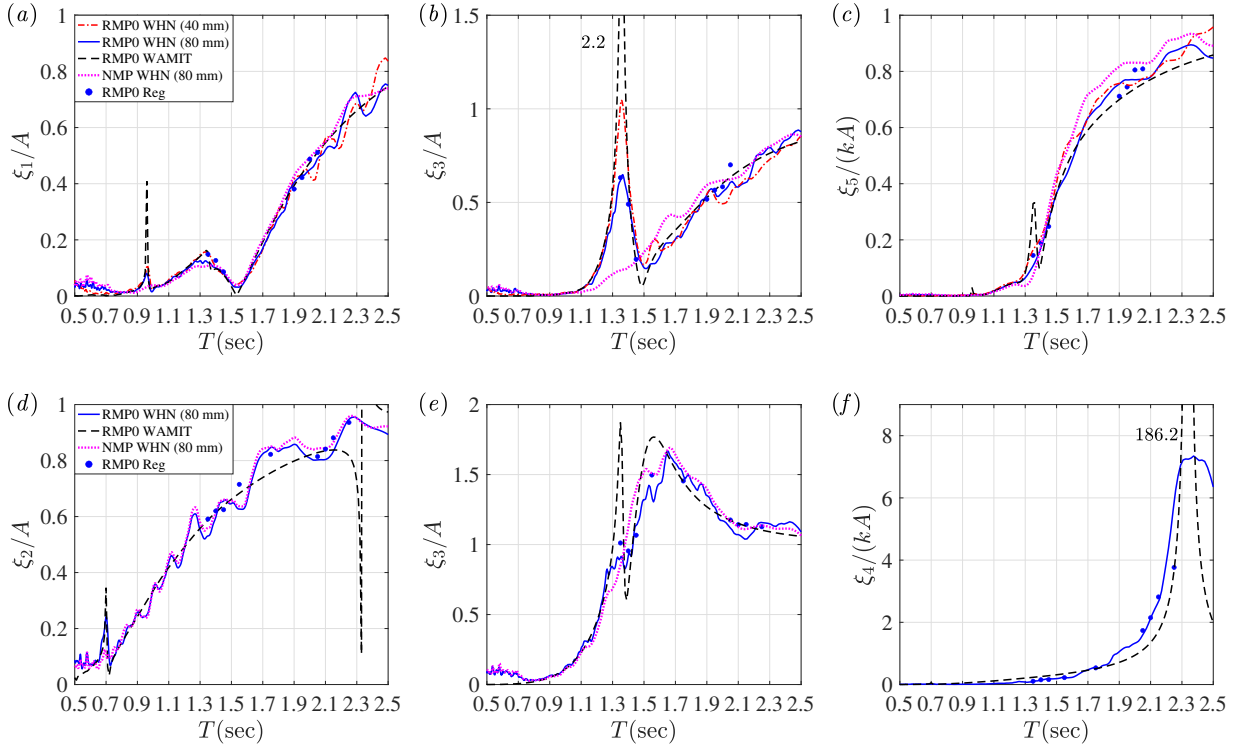


Figure 4: Motion RAOs of the ship with RMP0: (a) Surge, head wave; (b) Heave, head wave; (c) Pitch, head wave; (d) Sway, beam wave; (e) Heave, beam wave; (f) Roll, beam wave.

under head and beam waves. The measurements at WG1 positioned above the recess are analyzed in detail. The measurements at WG3 are utilized to study the response at the center of the moonpool. The measurements at WG5 and WG10 are adopted to examine the symmetry of the free-surface responses in head waves.

In general, the results of regular waves align with those of white-noise irregular waves with $H_s = 80$ mm. However, the free-surface RAO results of white-noise irregular waves with $H_s = 40$ mm are greater than those with $H_s = 80$ mm near piston resonance region, since a higher wave steepness can result in a larger damping value. The response is overestimated by WAMIT near the resonance region owing to the neglect of viscosity. In the non-resonant regions, the predictions by WAMIT generally agree well with the experimental results.

Fig. 3(a) illustrates the piston-mode resonance around ($T = 1.36$ s) and the first longitudinal sloshing response ($T = 0.98$ s) under head waves. In addition, the first transverse sloshing response ($T = 0.69$ s) is observed in the white-noise test results, which can be attributed to the non-trivial roll motion. However, this response is not observed in the results predicted by WAMIT due to symmetric configurations under head waves. Fig. 3(b) illustrates the responses measured at WG3 in different conditions. The first longitudinal sloshing mode ($T = 0.98$ s) is not observed since WG3 is located at the center of the moonpool. Fig. 3(c) shows that the free-surface responses at WG1 and WG10 are symmetric under head waves. Fig. 3(d) shows that the response amplitude at WG1 caused by the piston mode is smaller under beam waves than the head wave scenario. In addition, as illustrated in Fig. 3(d)-(f), a hump in the moonpool response is observed, which can be induced by the roll resonance ($T = 2.31$ s).

Fig. 4 illustrates the motion responses of the ship with a clean moonpool (RMP0) under head and beam waves. As shown in Fig. 4(a), the first longitudinal sloshing ($T = 0.98$ s) induces a peak in surge RAOs under head waves, whereas the piston-mode resonance ($T = 1.36$ s) has little effect on surge motion. Fig. 4(b) indicates that the piston-mode resonance causes a peak in the heave motion compared to the NMP case. Fig. 4(c) shows that the piston-mode resonance has a little effect on the pitch motion, because RMP0 is placed near the ship center. Fig. 4(d) illustrates the sway motion RAOs under beam waves. It is observed that the first transverse sloshing ($T = 0.69$ s) affects the sway motion. Fig. 4(e) shows that the piston mode has a minor impact on the heave motion under beam waves, which is different from the results under head wave, demonstrating the influence of wave direction on the coupled response between the ship and RMP0. Fig. 4(f) shows that the roll response is significantly overestimated by WAMIT near the roll resonant period of 2.31 s due to the neglect of the viscous damping effect.

Fig. 5 presents the free-surface response RAOs at WGs inside RMP4, which has the longest recess, as well as the surge, heave and pitch motion RAOs of the ship in head wave. By comparing Fig. 3(a) and Fig. 5(a), it is evident that the piston-mode period for RMP4 is larger compared to RMP0. In contrast, sloshing mode periods for RMP0 and RMP4 are almost the same. As shown in panel (a), near the piston-mode resonance, the results in regular waves for RMP4 are lower than those in white-noise irregular waves ($H_s = 80$ mm) due to enhanced viscous damping. In contrast, the results under regular waves for RMP0 agree well with those in

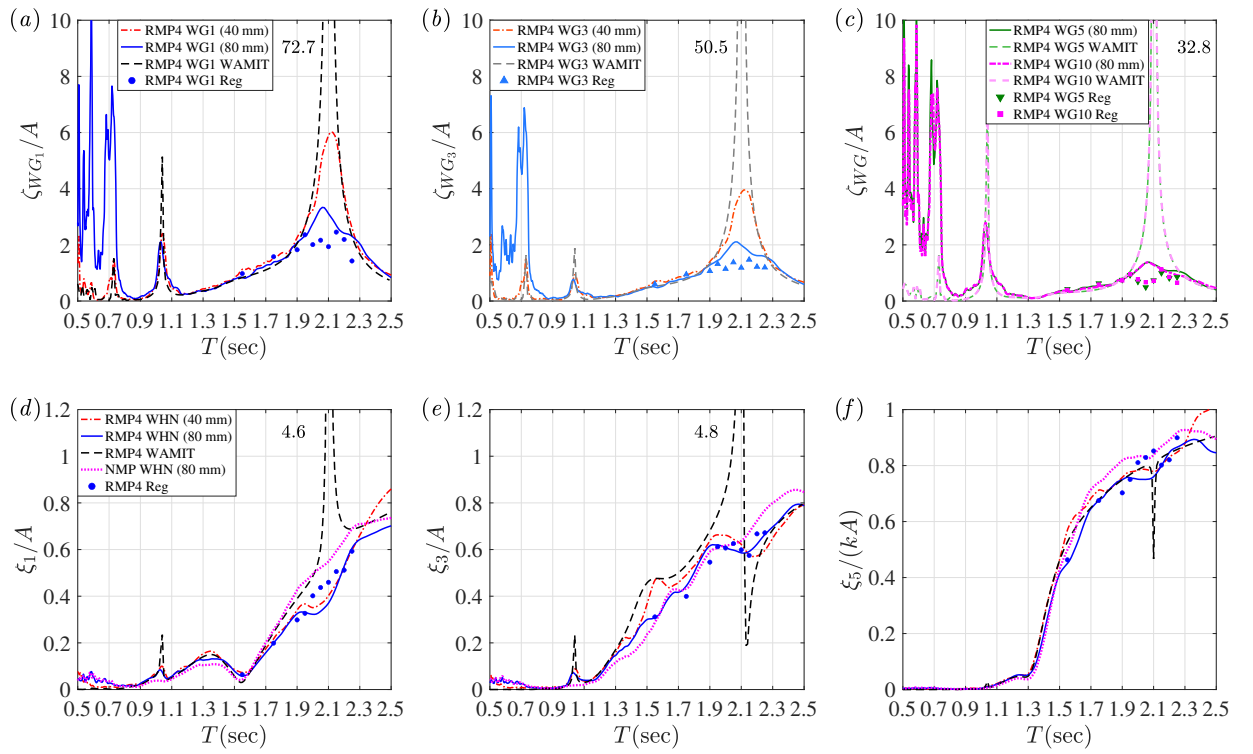


Figure 5: Motion RAOs of the ship with RMP4 and free-surface response RAOs at different WGs in head wave: (a) WG1; (b) WG3; (c) WG5 and WG10. (d) Surge; (e) Heave; (f) Pitch.

white-noise irregular waves ($H_s = 80$ mm). This is because RMP4 has an extra recess edge compared to RMP0, which can cause flow separation and induce more viscous damping.

Fig. 5(b) shows that the behavior of the free-surface RAO at WG3 is similar to that at WG1, while the piston-mode response magnitude at WG3 is relatively smaller. By comparing panels (a) and (c) in Fig. 5, it is observed that the free-surface response at WG5 is relatively lower than that at WG1, which is consistent with the modal shape of the piston-mode resonance by potential flow method (Molin, 2017).

Regarding the ship motion response, experimental results in Fig. 5(d) show that the piston mode resonance ($T = 2.10$ s) induces a downward hump in the surge motion, which is not evident in the RMP0 case. This is due to the presence of the recess. In Fig. 5(e), the heave motion responses from the experiments are compared with WAMIT results. The comparison shows that the effect of the piston-mode resonance on the heave motion is suppressed by the viscous damping, only showing a small hump in the experimental results near the period of 1.92 s. This is different with the results of RMP0, where the heave response shows a pronounced peak near the piston-mode resonance. In addition, the WAMIT results illustrated in Fig. 5(f) show that the piston-mode resonance leads to a decrease in pitch response. However, this effect is nearly negligible in the experimental results due to the viscous damping effects. More extensive analyses will be presented at the workshop.

Acknowledgement

The present work is sponsored by the National Natural Science Foundation of China under Grant No. 52171269.

References

- MOLIN, B. 2001 On the piston and sloshing modes in moonpools. *J. Fluid Mech.* **430**, 27–50.
- MOLIN, B. 2017 On natural modes in moonpools with recesses. *Appl. Ocean Res.* **67**, 1–8.
- MOLIN, B., ZHANG, X., HUANG, H. & REMY, F. 2018 On natural modes in moonpools and gaps in finite depth. *J. Fluid Mech.* **873**, 571–586.
- SENTHURAN, R., KRISTIANSEN, T., MOLIN, B. & OMMANI, B. 2020 Coupled vessel and moonpool responses in regular and irregular waves. *Appl. Ocean Res.* **96**, 102010.
- XU, X., ZHANG, X., CHU, B. & HUANG, H. 2020 On natural frequencies of three-dimensional moonpool of vessels in the fixed and free-floating conditions. *Ocean Eng.* **195**, 106656.
- ZHANG, X., HUANG, H. & SONG, X. 2019 On natural frequencies and modal shapes in two-dimensional asymmetric and symmetric moonpools in finite water depth. *Appl. Ocean Res.* **82**, 117–129.
- ZHANG, X. & LI, Z. 2022 Natural frequencies and modal shapes of three-dimensional moonpool with recess in infinite-depth and finite-depth waters. *Appl. Ocean Res.* **118**, 102921.